Shahrood University of Technology
Iranian Society of Mining Engineering (IRSME)
Journal of Mining and Environment (JME)
journal homepage: www.jme.shahroodut.ac.ir
THOMSON REUTERS
Vol. 10, No. 2, 2019, 493-505.
DOI: 10.22044/jme.2019.7902.1655

Using a combination of genetic algorithm and particle swarm optimization algorithm for GEMTIP modeling of spectral-induced polarization data

F. Sharifi, A.R. Arab Amiri* and A. Kamkar Rouhani

Faculty of Mining, Petroleum & Geophysics Engineering, Shahrood University of Technology, Shahrood, Iran

Received 26 December 2018; received in revised form 17 January 2019; accepted 12 February 2019

Keywords

Generalized Effective-Medium Theory of Induced Polarization

Genetic Algorithm

Particle Swarm Optimization

Spectral-Induced Polarization

Abstract

The generalized effective-medium theory of induced polarization (GEMTIP) is a newly developed relaxation model that incorporates the petro-physical and structural characteristics of polarizable rocks in the grain/porous scale to model their complex resistivity/conductivity spectra. The inversion of the GEMTIP relaxation model parameter from spectral-induced polarization data is a challenging issue because of the highly non-linear dependency of the observed data on the model parameter and non-uniqueness of the problem. To solve these problems as well as scape the local minima of the highly complicated cost function, the genetic algorithm (GA) can be applied but it has proven to be time-intensive computationally. However, this drawback can be resolved by incorporating a faster algorithm, e.g. particle swarm optimization (PSO). The aim of this work is to investigate whether recovering the model parameter of the ellipsoidal GEMTIP model from SIP data using the combined GA and PSO algorithms is possible. To achieve this aim, we set the best calculated individuals using GA as the search space of PSO, and then the best location achieved by PSO in each iteration is assigned as the updated model parameters. The results of our research work reveal that the model parameters can effectively be recovered using the approach proposed in this paper but the time constant of a noisy data that arises from the adverse dependency of this parameter on the ellipticity of a polarizable grain. Moreover, the execution time of the ellipsoidal GEMTIP modeling of complex resistivity data can be significantly improved using the proposed algorithm.

1. Introduction

The Spectral-induced polarization (SIP) has been the focus of interest because of its efficiency for characterization and discrimination of the induced polarization (IP) sources in the wide range of geoscience fields comprising mineral [1, 2] and oil [3] exploration, environmental and groundwater studies [4], CO_2 storage monitoring [5], and so on.

In the framework of this method, the effective conductivities/resistivities of inhomogeneous rock samples/formations associated with the IP sources are usually frequency-dependent and complex-valued [1, 2], and the quntitative interpretation of the acquired SIP data is performed using the relaxation models.

The most common relaxation models are the generalized effective-medium theory of induced polarization (GEMTIP) [1] and Cole-Cole [2] models. The Cole-Cole model describes the bulk resistivity of rocks and does not consider the rock composition but the GEMTIP model is developed based on the effective-medium theory to reveal the relationship between the rock composition and the complex resistivity/conductivity spectrum [1, 6, 7]. Therefore, in order to investigate the petro-physical characteristics of rocks using the complex resistivity/conductivity spectrum, the inverse modeling of the GEMTIP relaxation model has to be performed. In the last decade some researchers have made efforts to recover

* Corresponding author: alirezaarabamiri@yahoo.com (A.R. Arab Amiri).

either spherical or ellipsoidal GEMTIP model parameter from SIP data using regularized conjugate-gradient [6-9] and extensive line search [7, 10] algorithms. Both of these algorithms are local-search techniques and require a very good initial solution close to the true model for a successful convergence [11]. Therefore, Lin et al. [12] have developed a hybrid method based on the genetic algorithm (GA) and simulated annealing (SA) in conjunction with the regularized conjugate gradient method (hybrid SAAGA-RCG) for GEMTIP modeling of complex resistivity data. However, it has been demonstrated that the convergence rate of both GA and SA are significantly slow [12, 13]. On the other hand, a comparison between SA and particle swarm optimization (PSO) has indicated that PSO may achieve a better success with substantially improvement of the execution time because of the smaller number of function evaluations required for convergence [14-16]. Therefore, in this research work, in order to speed-up the convergence of the global search, we incorporated PSO into GA (CGAPSO) to recover the model parameters of highly complicated ellipsoidal GEMTIP relaxation model from SIP data in the MATLAB environment. To implement this hybrid method, we set up the best individuals provided by GA as a search space of PSO technique. Thereby, we applied the CGAPSO algorithm to invert both the free noise and noisy synthetic SIP data. The results of our approach indicated that the model parameters of ellipsoidal GEMTIP could be well-recovered from the synthetic data but the time constant or ellipticity. It may be related to the mutual adverse correlation between these parameters as both of them can shift the frequency of occurrence the maximum point of imaginary part of complex resistivity/conductivity.

We found that the ellipsoidal GEMTIP modeling using CGAPSO could be performed at least 4.9 times faster compared to the hybrid SAAGA-RCG.

2. Spectral inductive polarization method

The SIP method is based on the frequency dependency of resistivities/conductivities of rocks associated with IP mechanisms (e.g. membrane polarization, electrode polarization) [17].

SIP measurement is conducted by injecting the harmonic alternative current in a wide range of frequencies from 0.01 to 10^4 Hz and measuring the potential, which in the presence of the IP effect is a complex value. Therefore, the apparent resistivity is a complex value and is considered as an induced polarization effect [5, 17]. It is given by:

$$\rho^*(\omega) = \rho'(\omega) + i\,\rho''(\omega) \tag{1}$$

where ρ' and ρ'' denote, respectively, the real and imaginary parts of the apparent resistivity and ω is the angular frequency.

The amplitude and phase-shift of the apparent resistivity obtained from the SIP measurement are related by Equation (2). The amplitude and phase-shift of the apparent resistivity can also be calculated using Equation (3).

$$\rho^*(\omega) = \left|\rho^*\right| e^{i\varphi} \tag{2}$$

$$\left|\rho^*\right| = \sqrt{(\rho')^2 + (\rho'')^2}$$

$$\tan(\varphi) = \frac{\rho''}{\rho'} \tag{3}$$

2.1. SIP data uncertainties

There are significant challenges to obtain reliable laboratory SIP data. To reduce the error of SIP measurements, a considerable attention should be paid to the sample preparation, size of sample holder, temperature of SIP cell, sample saturation, time duration of saturation, and calibration of the instrument [4].

The SIP measurements are usually conducted using the frequency-domain instruments, which suffer from the capacitive coupling above the frequency of 1 KHz depending on the conductivity of rock sample, cable arrangement, and operational frequency. However, several efforts have been made in order to reduce the effect of this undesired signal, e.g. fitting a relaxation model to the EM coupling data [2], taking both the electromagnetic coupling and IP effect modeling into account using the dipole-dipole electrode array and connecting each electrode using the individual shielded cable [4]. However, in this research work we assumed that the SIP data was acquired with high-quality instruments and that they were decoupled.

3. GEMTIP relaxation model

The GEMTIP relaxation model has been developed by Zhdanov [1]. In the context of this relaxation model, the heterogeneous rock formation is assumed to be equivalent to a composite model formed by a homogeneous host material filled with grains of arbitrary shape and

resistivity/conductivity [1, 9]. The effective resistivity of the composite model is mathematically expressed by:

$$\rho_e = \rho_0 \left[1 + \sum_{l=1}^{N} \sum_{a=x,y,z} \frac{f_l}{3\gamma_{l\alpha}} \left(1 - \frac{1}{1+(i\omega\tau_l)^{c_l} \frac{\gamma_{l\alpha}}{2\bar{a}_l \lambda_{l\alpha}}}\right) \right]^{-1} \quad (4)$$

where ρ_0 is a DC resistivity, f_l is a volume fraction of grains, $\gamma_{l\alpha}$ and $\lambda_{l\alpha}$ are the volume and surface depolarization parameters of the ellipsoidal grain, $\bar{a}_l$ is an average value for the equatorial (b) and polar (a) radii, τ_l is a time constant, c_l is a frequency-dependent of l^{th} grain, and $\omega = 2\pi f$ is an angular frequency.

The volume depolarization is calculated for prolate spheroid ($a>b$) and oblate spheroid ($a<b$) using Equations (5) and (6), respectively [18].

$$\gamma_l = \frac{1-\varepsilon_l^2}{\varepsilon_l^3}(\tanh^{-1}\varepsilon_l - \varepsilon_l)$$

where (5)

$$\varepsilon_l = \sqrt{1-e_l^{\,2}}$$

$$\gamma_l = \frac{1+\varepsilon_l^2}{\varepsilon_l^3}(\varepsilon_l - \tan^{-1}\varepsilon_l)$$

where (6)

$$\varepsilon_l = \sqrt{e_l^{\,2}-1}$$

In Equations (5) and (6), ε is an eccentricity and e_l is an ellipticity of the grains.

To determine the volume depolarization components, the following condition must be satisfied [18]:

$$\gamma_x = \gamma_y = \frac{1}{2}(1-\gamma_l) \quad (7)$$

$$\gamma_z = \gamma \quad (8)$$

The surface depolarization components are calculated as follows [18]:

$$\lambda_x = \lambda_y = \frac{ab^3}{2}\int_0^b \frac{\left[2a^2b^2 - (b^2-a^2)z^2\right](b^2-z^2)}{\left[a^2b^2+(b^2-a^2)z^2\right]^{5/2}\sqrt{b^4-(b^2-a^2)z^2}}dz \quad (9)$$

$$\lambda_z = ba^3\int_0^b \frac{\left[3b^4 - b^2a^2 - (b^2-a^2)z^2\right]z^2}{\left[a^2b^2+(b^2-a^2)z^2\right]^{5/2}\sqrt{b^4-(b^2-a^2)z^2}}dz \quad (10)$$

4. Modeling

For recovering the petro-physical and electrical parameters of the polarizable rock from SIP data, we used the ellipsoidal GEMTIP relaxation model as a forward operator, and then inverted the model parameters using the CGAPSO algorithm.

4.1. Forward operator

In order to evaluate the effect of varying the model parameters of the ellipsoidal GEMTIP model (e.g. DC resistivity, volume fraction, ellipticity, time constant, and frequency dependence of grains) on a complex resistivity/conductivity spectrum, we considered the two-phase synthetic models, and then modeled the SIP data in response to changing the GEMTIP model parameters (Table 1). The modeling results are shown in Figures 1 to 5.

Table 1. Two-phase ellipsoidal GEMTIP parameters of synthetic models [7].

Model	DC resistivity	Volume fraction (%)	Ellipticity	Time constant	Frequency dependent
Model 1	50-500	10	4	0.5	0.5
Model 2	50	1-10	4	0.5	0.5
Model 3	50	10	0.125-8	0.5	0.5
Model 4	50	10	4	0.001-10	0.5
Model 5	50	10	4	0.5	0.01-0.9

4.1.1. DC resistivity

The recovered DC resistivity from the GEMTIP relaxation model corresponds to the matrix resistivity of the polarizable rock. The effect of varying the DC resistivity on the GEMTIP response, while the other model parameters are kept constant (model 1), is depicted in Figure 1. As it can be seen in this figure, the DC resistivity affects both the real and imaginary parts of the complex conductivity spectra significantly. Increasing the DC resistivity (decreasing its reciprocal, i.e. conductivity) reduces the amplitude of both the real and imaginary parts of the complex conductivity spectra.

4.1.2. Volume fraction

The ellipsoidal GEMTIP response of model 2 (see Table 1) is presented in Figure 2, which shows that how varying the volume fraction of polarizable grains can affect the complex

conductivity spectrum. As the figure indicates, increasing the volume fraction enhances the amplitude of both the real and imaginary parts of the complex conductivity.

4.1.3. Ellipticity

Recovering the ellipticity of polarizable grain/pore spaces of a rock provides information about their shape and structure, which could be very useful in a petro-physical study. The response of the elliptical GEMTIP with regard to varying the ellipticity of polarizable grain is simulated using the parameters of model 3 given in Table 1.

Increasing the ellipticity of polarizable grains, as shown in Figure 3, intensifies the amplitude of the real part of complex conductivity for both the prolate (e < 1) and oblate (e > 1) elliptical shape grains. However, the intensity of the imaginary part gets higher as the ellipticity of prolate grains decrease, and it gets stronger as the ellipticity of oblate grains increases. Moreover, varying the ellipticity shifts the maximum imaginary point.

4.1.4. Time constant

The time constant parameter of the GEMTIP relaxation model is directly dependent on the size of a polarizable grain/pore. In other words, a large time constant value corresponds to the large grain size, and vice versa.

The effect of varying the time constant on the complex conductivity response is modeled by applying the ellipsoidal GEMTIP to the synthetic model 4 (see Table 1). The complex conductivity spectra obtained are shown in Figure 4.

This Figure indicates that as the time constant increases, the amplitude of the real part is intensified and the maximum point of the imaginary part shifts toward lower frequencies.

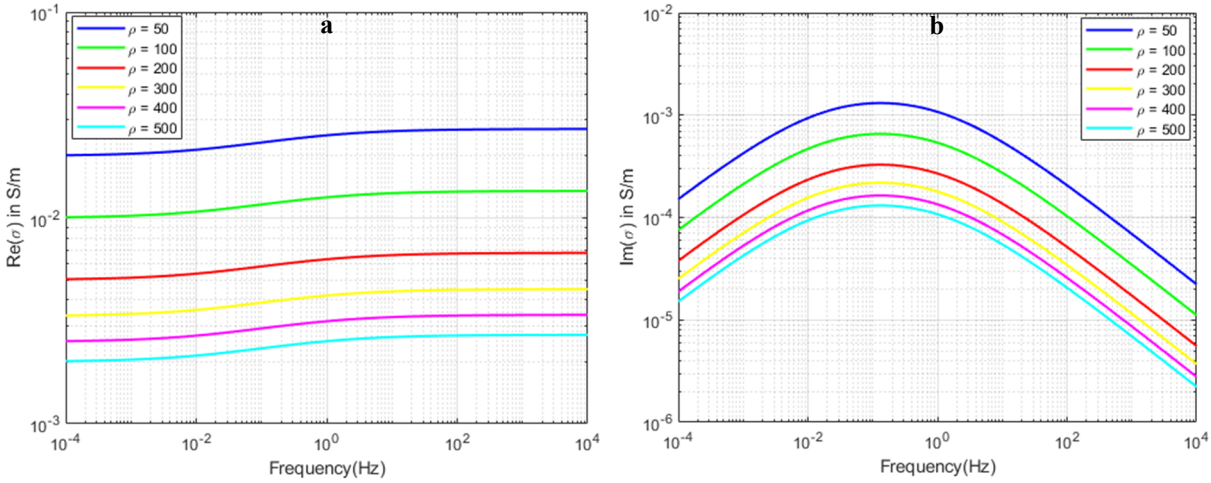

Figure 1. The effect of varying DC resistivity on the real (a) and imaginary (b) parts of the complex conductivity obtained from a two-phase ellipsoidal GEMTIP modeling.

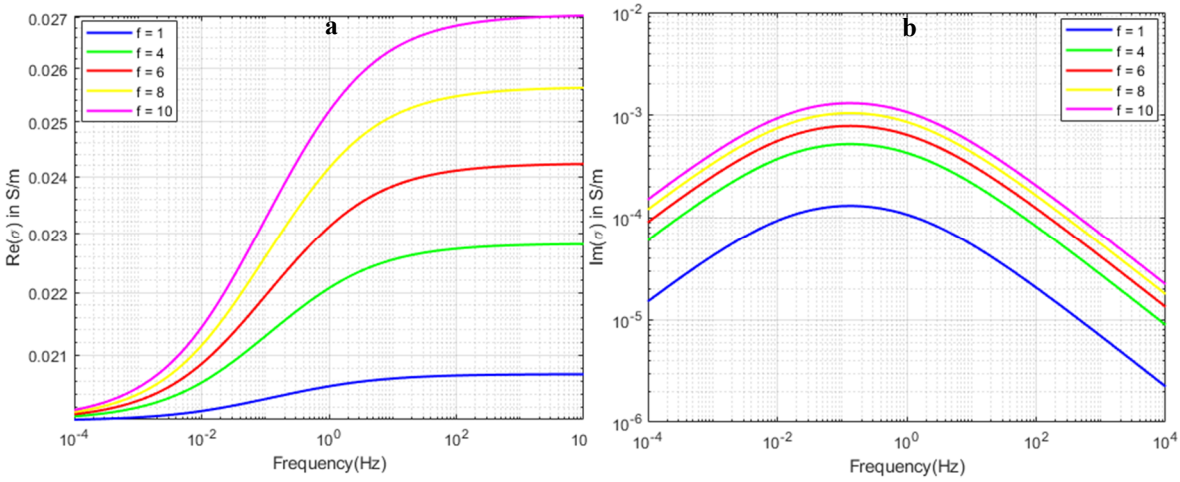

Figure 2. The effect of varying volume fraction of polarizable grains on the real (a) and imaginary (b) parts of the complex conductivity obtained from a two-phase ellipsoidal GEMTIP modeling.

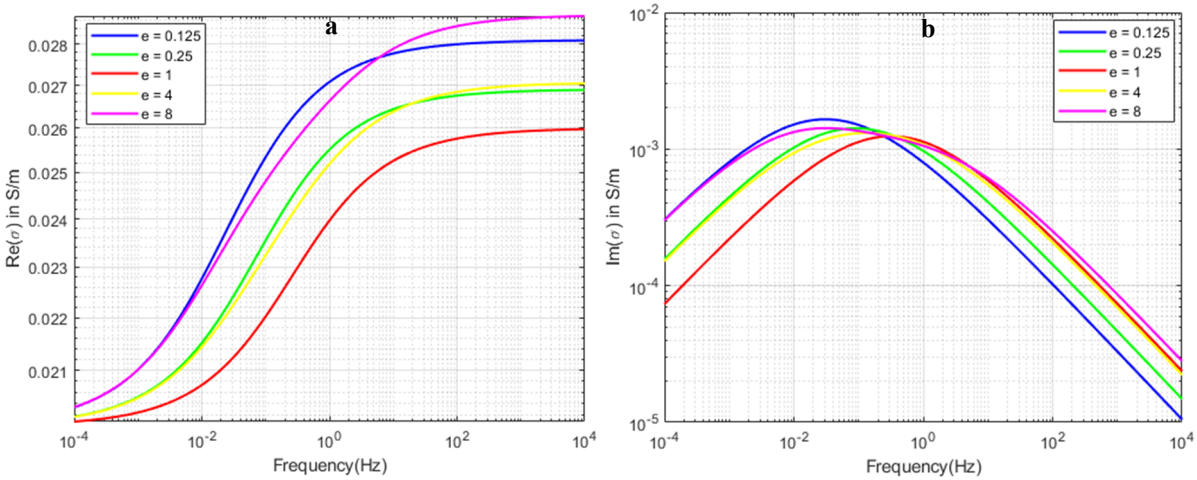

Figure 3. The effect of varying ellipticity of polarizable grains on the real (a) and imaginary (b) parts of the complex conductivity obtained from a two-phase ellipsoidal GEMTIP modeling.

4.1.5. Frequency dependent

The frequency-dependent parameter reflects the inhomogeneity (grain-size distribution) of the polarizable grains included in the rock formations. As the inhomogeneity increases, the frequency dependence decreases, and vice versa.

The effect of varying the frequency dependence on the response obtained from the two-phase ellipsoidal GEMTIP modeling is demonstrated in Figure 5. As it can be seen in the real part of the complex conductivity spectrum, in the left side of the cross point (CP), the amplitudes of the spectra decrease, while in the right side of the CP point, it represents an opposite behavior. However, the amplitude of the imaginary part increases as the frequency-dependence value increases.

4.2. Inverse modeling

The relationship between the model parameters and the measured SIP data is given as follows:

$$d = G(m) \tag{11}$$

where $m = [\rho_0, e_l, \tau_l, c_l, f_l, a_l]$ is the unknown model parameter vector of size N_m, $d = [\rho_e(\omega_1), \rho_e(\omega_2), \ldots, \rho_e(\omega_n)]$ is the observed data vector, and G is the ellipsoidal GEMTIP forward operator.

In order to find the model parameters of GEMTIP, one has to invert Equation (11). To achieve this aim, we implemented a CGAPSO algorithm to recover a three-phase ellipsoidal GEMTIP model proposed by Fu [7] and Lin et al. [12].

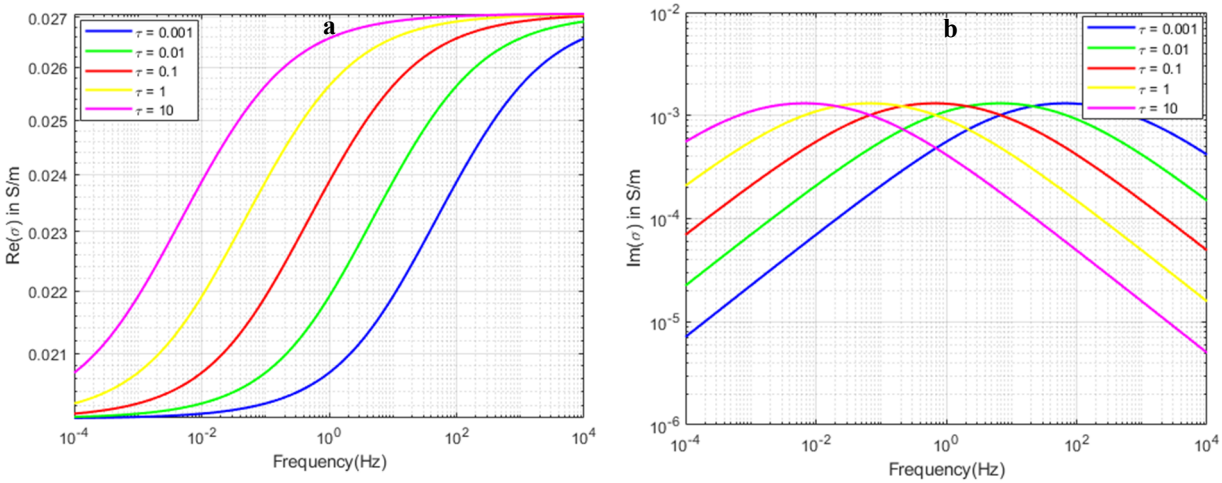

Figure 4. The effect of varying time constant of polarizable grains on the real (a) and imaginary (b) parts of the complex conductivity obtained from a two-phase ellipsoidal GEMTIP modeling.

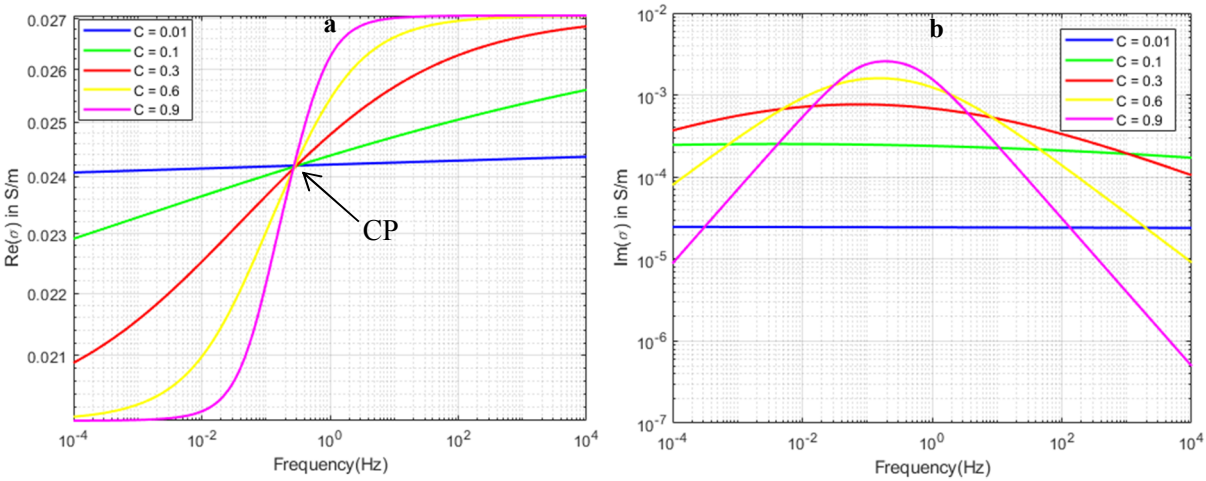

Figure 5. The effect of varying frequency-dependence of polarizable grains on the real (a) and imaginary (b) parts of the complex conductivity obtained from a two-phase ellipsoidal GEMTIP modeling.

4.2.1. CGAPSO algorithm

GA is a common method in the academic and industrial sectors mainly because of its intuitiveness, ease of implementation, and ability to effectively solve the highly non-linear, mixed integer optimization problems [13]. However, it suffers from an expensive computational drawback. Therefore, in order to speed-up the convergence to the global minimum, a reliable algorithm can be combined with GA. PSO has been proven to be computationally more efficient than GA to obtain the high quality solution, and the computational effort required by PSO to achieve a solution is less than the effort required to achieve the same quality of solution by GA [13, 19]. Therefore, we incorporated PSO into GA in order to take the advantages of both algorithms.

The CGAPSO algorithm in each iteration uses both the GA and PSO algorithms (Figure 6) to find the best solution, which represents the lowest value of a cost function (the highest value of fitness). The cost function is calculated using the following equation:

$$\varphi(m) = \left(d^{obs} - G(m)\right) / d^{obs} / \sqrt{n-1} \qquad (12)$$

where φ is the cost function, d^{obs} is the observed data, and n is the number of measured data.

4.2.1.1. GA

GA is a global optimization technique inspired by the processes of biological evolution [13]. The main steps of GA are initialization, evaluation, reproduction (selection), cross-over, and mutation. The algorithm is implemented for the three-phase ellipsoidal GEMTIP model as follows [13]:

1- Initialization: In this step, a random population of size N_{pop} with the chromosome (parameter) values between the lower bound m_i^- and upper bound m_i^+ generated. Each row of the population calls an individual, which represents a possible vector of m for the GEMTIP model.

The population size (N_{pop}) has a significant influence on the GA performance. A larger initial diversity of the population allows the larger parts of the search space to be covered. Although increasing N_{pop} increases the computation time in each iteration, it may lead to less iterations to achieve an optimal solution compared to a small N_{pop}. However, it has been found that it could not be greater than 2^{Nm} (in the current case, $N_m = 9$) to avoid a duplicated chromosome. Therefore, a maximum size of population in our case could not be greater than 2^9, which means that the search space of each parameter of the ellipsoidal GEMTIP model, maximally, can be divided into 2^9 parts, varying between their upper bound and lower bound [13].

2- Evaluation: In this phase, calculation of the fitness function is carried out. The fitness of the k^{th} individual of the population can be obtained using the following equation [12]:

$$f(k) = 1 / \sum_{l=1}^{N_{pop}} \exp\left(\varphi(k) - \varphi(l)\right) \qquad (13)$$

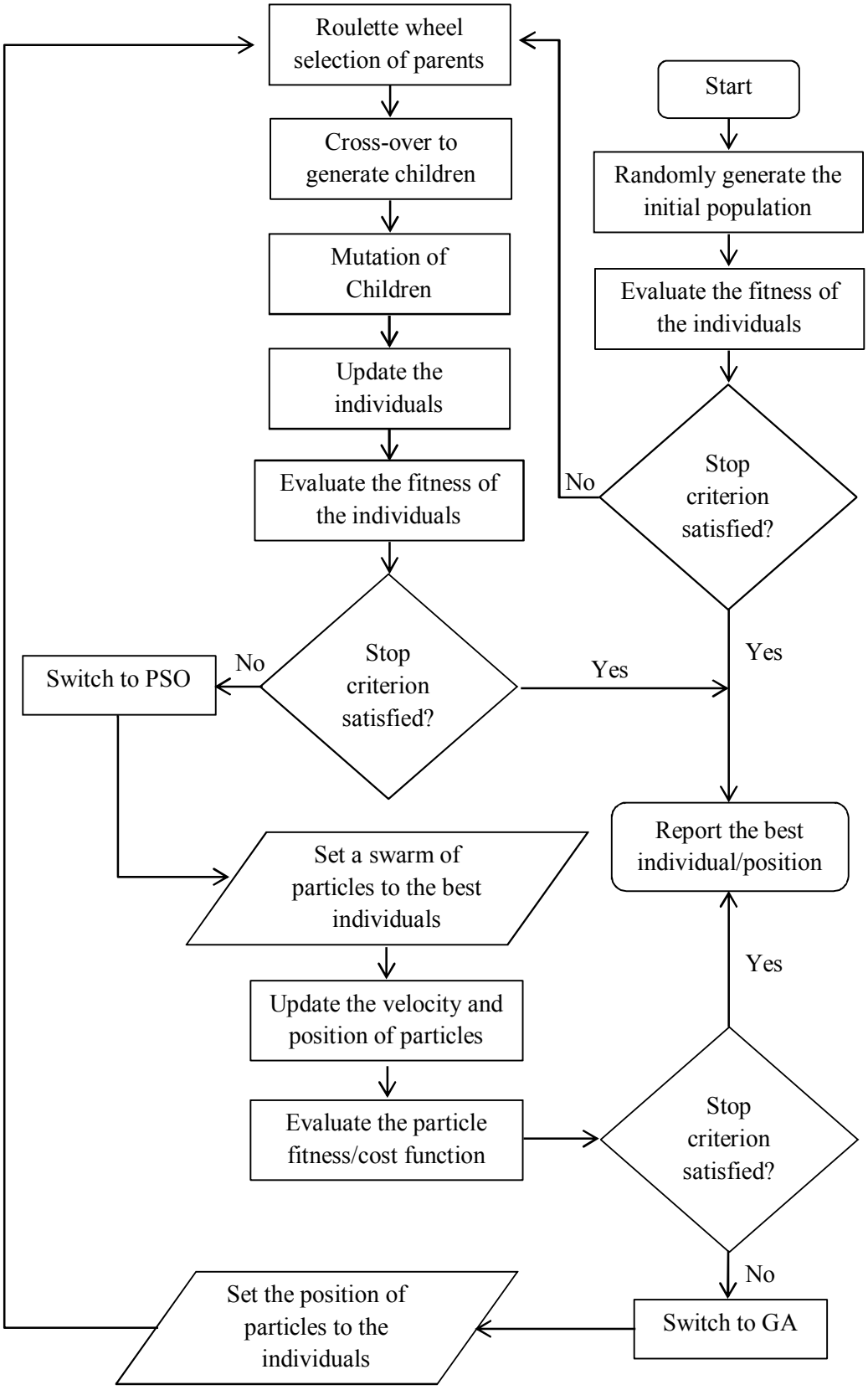

Figure 6. A flowchart of the CGAPSO algorithm.

3- Reproduction: In this step, selection of the individuals to be assigned as parents for the cross-over step using the roulette wheel selection operator is made using the following expressions [13]:

$$P_k = \frac{f(k)}{\sum_{k=1}^{N_{pop}} f(k)} \quad (14)$$

$$C_k = \sum_{j=1}^{k} P_j \quad (15)$$

where C_k is a cumulative sum of the probabilities of the k^{th} individual. To find the index of the individual to be contributed in the cross-over, we look for the index of a randomly generated number, $0 \le r \le 1$, where $r \le C_k$.

4- Cross-over and mutation: Both the cross-over and mutation operators are used to produce a new population by making a change into the selected individuals. Cross-over causes the exchange of some information between the paired individuals, and thereby, generating new pairs of model parameters [13].

Mutation is the random alteration of a model parameter. It can be conducted through changing the randomly selected model parameter with a pre-determined mutation probability [13].

We set the probability of cross-over and mutation to 0.7 and 0.2, respectively.

The mutated model parameter is updated using the following equation:

$$m_j^{mut} = m_j^{old} + \beta.N(0,1) \quad (16)$$

where N is the standard normal distribution, and β is the step length, which is calculated using the following mathematical expression:

$$\beta = \alpha(m_{max} - m_{min}) \quad (17)$$

where α is a coefficient, which is considered to be 0.1 in this research work.

4.2.1.2. PSO

PSO is inspired from the social behavior of real swarms (e.g. bird flocking or fish schooling) when they are looking for food sources [20].

It has been shown in a number of empirical studies that PSO has the ability to find an optimal solution with small swarm sizes of 10 to 30 particles [21]. However, the optimal size of the swarm is problem-dependent. Furthermore, thumb's rule suggests 3 to 4 times the number of model parameters (particles) for the swarm size. However, in conjunction with GA to perform the CGAPSO algorithm, we have found that N_{pop} of size 50 is suitable for our case from the viewpoint of both the GA performance and relatively fast convergence to the global optimum point.

In the framework of CGAPSO, the updated population using GA is assigned as the search space of PSO in each iteration.

For implementing PSO, the particles iteratively change their positions and generate a sequence of sub-iterations that stop when an appropriate termination criterion is met including either the problem that has been solved within a desired accuracy or that no further progress can be made [13, 14].

The distance that each particle travels toward its next position is found via the equation $x = v.\Delta t$, where v is the velocity calculated for particle m at sub-iteration t, as follows [13, 19]:

$$v_i^c = k[v_i^{c-1} + w_1.rand(N_m)(m_i^l - m_i^c) + w_2.ran \quad (18)$$

The model parameter is updated according to the following expression:

$$m_i^{c+1} = m_i^c + v_i^c \quad (19)$$

where m_i^c is the current model parameter, v_i^c is the current velocity, m_i^l the best model parameter, m_g is the best model parameter that is found by the swarm before the current implementation, and w_1 and w_2 are the constriction coefficients [22].

k is the constriction factor, which is calculated as follows:

$$k = \frac{2}{\left|2 - \varphi - \sqrt{\varphi^2 - 4\varphi}\right|} \quad (20)$$

where $\varphi = w_1 + w_2$, $\varphi > 4$

The condition $\varphi > 4$ ensures the stability of the algorithm. Therefore, when the constriction factor is used, φ is set to 4.1 (i.e. $w_1 = 2.05$ and $c_2 = 2.05$), and k is thus 0.729 [22].

In order to control the convergence of the algorithm, the velocity bounds have to be pre-defined as follow:

$$v_i^+ = (m_i^+ - m_i^-)/10$$

and (21)

$$v_i^- = -v_i^+$$

where v_i^+ and v_i^- are the upper and lower bounds of velocity, respectively.

5. Results and discussion

SIP is the most promising geophysical method that is used for IP source discrimination based on the frequency-dependent complex conductivity/resistivity. However, the quantitative interpretation of the SIP data is performed using the relaxation models. The parameters of the relaxation model are used for discrimination of the different types of rock formation, which is an important goal in the mineral and petroleum exploration, environmental and ground water study, and so on. One of the most common relaxation models is a well-known Cole-Cole model. However, this model describes the bulk resistivity and does not account for rock structure or composition directly. Furthermore, it has been proved that this relaxation model is a simplified expression of a newly developed GEMTIP relaxation model. The GEMTIP model allows the grain size and shape, conductivity/resistivity, porosity, anisotropy, polarizability, and mineral/fluid volume fraction to be incorporated in a physical-mathematical model of rocks. Regarding the ellipticity of IP sources, two versions of GEMTIP can be applied, spherical GEMTIP (e = 1) and ellipsoidal GEMTIP (e ≠ 1). Ellipsoidal GEMTI is a more complicated model that provides information about the shape of a polarizable grain. The importance of the model parameters of ellipsoidal GEMTIP is investigated in Figures 1 to 5. The results of our simulation using the ellipsoidal GEMTIP model show that higher values of conductivity of the matrix of rock sample (Figure 1) as well as a higher percentage of volume fraction of polarizable grain (Figure 2) cause a stronger SIP signal compared to the lower values for these parameters. Also varying the ellipticity of polarizable grain affects the complex conductivity obtained in a way that the greater amplitude of the real part of complex conductivity is correlated with higher values of ellipticity, although the amplitude of the imaginary part represents a different behavior in response to varying the ellipticity of both the prolate (e < 1) and oblate (e > 1) grains. For the prolate grains, it gets decreased with increase in the ellipticity but for the oblate grains, it shows an opposite behavior. Moreover, varying the ellipticity shifts the frequency of occurring maximum point of the imaginary part (Figure 3).

Time constant, in direct correlation, reflects the effect of varying the grain size on the complex conductivity data obtained. Therefore, based on Figure 4, the effect of polarizable coarse grain size is reflected in the lower frequency and the response of fine grains appears in higher frequencies.

The effect of grain size distribution (inhomogeneity) is modeled by the frequency-dependent parameter. The effect of increasing the inhomogeneity causes the frequency-dependence to decrease, and vice versa. In response to increasing the frequency dependence and homogeneity of grain size of polarizable grain, the amplitude of the real part in the right side of the cross point (CP) as well as the amplitude of the imaginary part of complex conductivity is increased, whereas the real part represents the opposite behavior in the left side of CP (Figure 5).

These features are used as a promising signature in geophysical SIP investigations. Therefore, it would be most persuasive to develop a reliable technique for recovering the model parameters of ellipsoidal GEMTIP. This relaxation model is highly non-linear and the corresponding cost function may be associated with multiple local minima. These challenges can be resolved by applying GA but it has been found to be highly time-consuming. In the other side, the PSO algorithm has been found to be able to speed-up the convergence to the global point as it requires a relatively small population size compared to GA. Therefore, we incorporated PSO into GA in order to take advantage of both algorithms for the ellipsoidal GEMTIP modeling of complex resistivity data.

In order to evaluate the performance of the CGAPSO algorithm for recovering the ellipsoidal GEMTIP model parameters from complex resistivity data, we have considered a three-phase ellipsoidal GEMTIP model, and then generated the synthetic complex resistivity data using Equation (4). Thereby, three sets of data including free noise data and noisy data with 0.5% and 3% of normal noise are obtained using the model parameters given in Table 2.

As outlined in Figure 7, including two polarizable grains with different ellipsoidal GEMTIP model parameters affected the real and imaginary parts and phase shift of complex resistivity. It inflected the real part spectrum in a frequency of 1 Hz. Also the imaginary part and phase shift of GEMTIP response is characterized by the occurrence of double peak spectra. Considering

the time constant and ellipticity values of the grains (see Table 2), the SIP effect of grain 1 (P1) appears at higher frequencies, whereas the corresponding peak of grain 2 (P2) takes place at lower frequencies.

To implement CGAPSO, we set the algorithm to reiterate GA and PSO two and three times, respectively, in each iteration of CGAPSO with N_{pop} of size 50.

To compare the performance of our approach with the recently developed hybrid SAAGA-RCG, we set the stop criterion of CGAPSO to the rms error of less than 0.5, which had been set in hybrid SAAGA-RCG. We executed the code for both the free noise data and noisy data with 0.5% normal noise. In the case of free noise data modelling, the algorithm stopped after 53 iteration of executing with the elapsed time of 33.17 s. However, in the case of modeling the noisy data with 0.5% noise, it terminated at the iteration number of 71 with the elapsed time of 44.92 s, whereas the number of iteration and elapsed time of execution of hybrid SAAGA-RCG for recovering the same model have been stated to be 228 and 220 s, respectively.

Afterward, we set the termination criterion to the number of iteration of 1000 for inversion of the free noise data and noisy data with 3% of normal noise. Thereby, the predicted ellipsoidal GEMTIP of free noise data is successfully fitted to the double-peak synthetic complex resistivity data (Figure 7a-c) with the rms error of 0.001% (Figure 8a), although in the case of inversion of noisy data, as it can be seen in Figure 7d-e, the predicted data is well-fitted to the double-peak synthetic complex resistivity data with the rms error of 2.8% (Figure 8b).

The recovered model parameters using the CGAPSO algorithm were tabulated in Table 3. As it can be found in this table, the model parameters are well-recovered but the time constant from noisy data. It may be related to the mutual adverse interaction between the time constant and ellipticity. As it can be seen in Figures 3 and 4, both the time constant and ellipticity shift the frequency of occurrence of the maximum IP. Therefore, the exchange between these parameters affects the recovered values of their counterparts.

Table 2. Three-phase ellipsoidal GEMTIP model parameters of synthetic models [7, 12].

Grain 1		Grain 2	
f_1	15%	f_2	10%
τ_1	0.01	τ_2	0.9
e_1	1	e_2	4
c_1	0.9	c_2	0.9
ρ_0 (ohm.m)		200	

Table 3. The recovered model parameters of the three-phase ellipsoidal GEMTIP model.

GEMTIP parameters	Free noise data	Noisy data (3% noise)
$\boldsymbol{\rho_0}$	200.00	199.96
$\boldsymbol{f_1}$	14.98%	12.07%
$\boldsymbol{\tau_1}$	0.00997	1.1410
$\boldsymbol{e_1}$	1.12	1.5711
$\boldsymbol{c_1}$	0.900	0.7854
$\boldsymbol{f_2}$	10.00%	12.43%
$\boldsymbol{\tau_2}$	0.8999	0.0053
$\boldsymbol{e_2}$	4.00	4.4818
$\boldsymbol{c_2}$	0.8999	0.9835

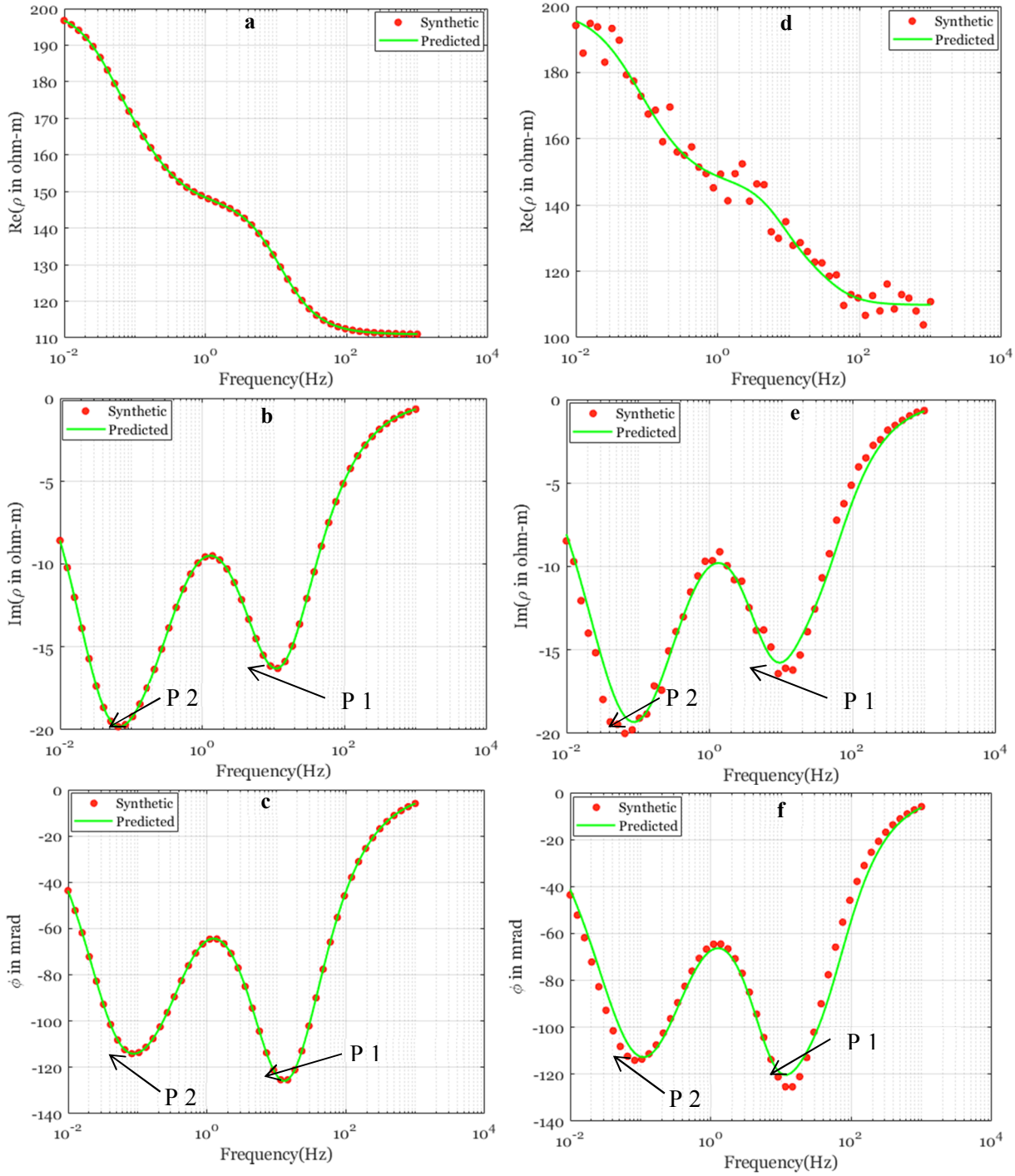

Figure 7. Real (a and d), imaginary (b and e), and phase shift (c and f) spectra of synthetic (red points) and recovered (green line) data obtained using the three-phase ellipsoidal GEMTIP modeling for free noise (a, b, and c) and noisy (d, e, and f) data.

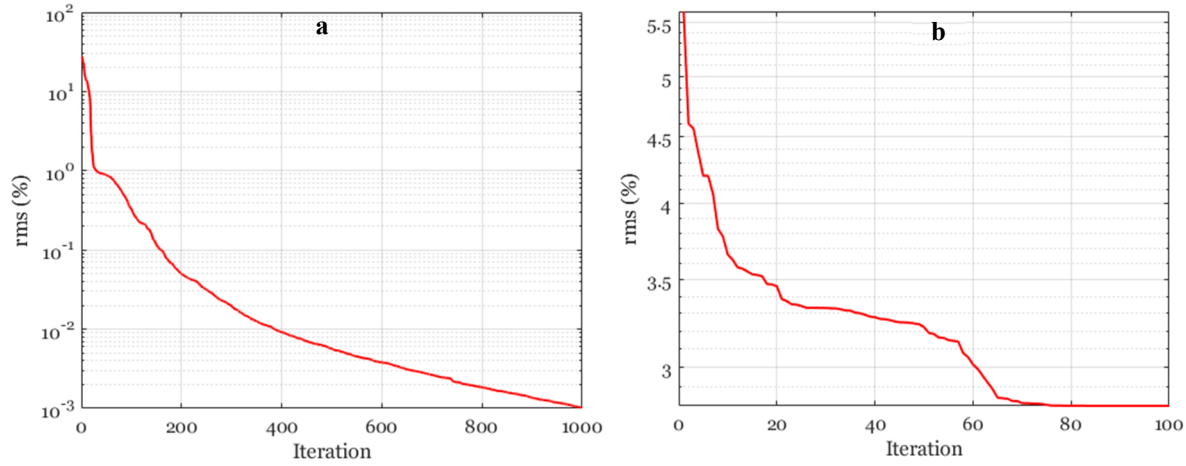

Figure 8. Convergence rate of the three-phase ellipsoidal GEMTIP inversion of free noise (a) and noisy (b) data using the CGAPSO algorithm.

6. Conclusions

In this work, we have implemented the ellipsoidal GEMTIP modeling of complex resistivity data. We applied a combined GA and PSO (CGAPSO) algorithm to recover the model parameters of three-phase ellipsoidal GEMTIP relaxation model from synthetic complex resistivity data. The promising results of this research work are outlined as follow:

-In the case of inverting the free noise data, the model parameters are well-recovered using the CGAPSO algorithm.

-In the case of GEMTIP modeling of the noisy data, the optimal recovering of the model parameters, except time constant, is achieved. This failure may arise from either the mutual interaction between the time constant and ellipticity or the noise pollution of the SIP data as it prevents the algorithm to converge to a smaller rms error.

-A significant degree of improvement in the time of execution for ellipsoidal GEMTIP modeling of SIP data is successfully achieved using the CGAPSO algorithm.

Acknowledgments

Authors gratefully acknowledges Dr. Alexander V. Gribenko for his kindly advices on the GEMTIP modeling. Also the authors gratefully thank reviewers for their comments and questions that helped us to improve the manuscript.

References

[1]. Zhdanov, M. (2008). Generalized effective-medium theory of induced polarization. Geophysics. 73 (5): F197-F211.

[2]. Pelton, W.H., Ward, S.H., Hallof, P.G., Sill, W.R. and Nelson, P.H. (1978). Mineral discrimination and removal of inductive coupling with multifrequency IP. Geophysics. 43 (3): 588-609.

[3]. Luo, Y. and Zhang, G. (1998). Theory and application of spectral induced polarization. Tulsa: Society of Exploration Geophysicists (SEG).

[4]. Kemna, A., Binley, A., Cassiani, G., Niederleithinger, E., Revil, A., Slater, L. and Zimmermann, E. (2012). An overview of the spectral induced polarization method for near-surface applications. Near Surf Geophys. 10 (6): 453-468.

[5]. Boerner, J.H., Herdegen, V., Repke, J.U. and Spitzer, K. (2016). Spectral induced polarization of the three-phase system CO_2-brine-sand under reservoir conditions. Geophys J Int. 208 (1): 289-305.

[6]. Phillips, C.R. (2010). Experimental study of the induced polarization effect using Cole-Cole and GEMTIP models (Master of Science dissertation, The University of Utah).

[7]. Fu, H. (2013). Interpretation of complex resistivity of rocks using GEMTIP analysis (Master of Science dissertation, The University of Utah).

[8]. Buist, S.I. (2009). Induced polarization effect in land and marine CSEM data: applications for hydrocarbon exploration (Master of Science dissertation, The University of Utah).

[9]. Burtman, V., Zhdanov, M.S. and Fu, H. (2014). Spectral induced polarization effect in unconventional reservoir rocks. SEG Technical Program Expanded Abstracts. pp. 907-911.

[10]. Burtman, V., Fu, H. and Zhdanov, M.S. (2014). Experimental Study of Induced Polarization Effect in Unconventional Reservoir Rocks. Geomaterials. 4 (04): 117.

[11]. Shaw, R. and Srivastava, S. (2007). Particle swarm optimization: A new tool to invert geophysical data. Geophysics, 72 (2): F75-F83.

[12]. Lin, W., Zhdanov, M.S., Burtman, V. and Gribenko, A. (2015). GEMTIP inversion of complex resistivity data using a hybrid method based on a genetic algorithm with simulated annealing and regularized conjugate gradient method. SEG Technical Program Expanded Abstracts. pp. 952-956.

[13]. Sen, M.K. and Stoffa, P.L. (2013). Global optimization methods in geophysical inversion. Cambridge University Press. 289 P.

[14]. Ethni, S.A., Zahawi, B., Giaouris, D. and Acarnley, P.P. (2009). Comparison of particle swarm and simulated annealing algorithms for induction motor fault identification. 7th IEEE International Conference on Industrial Informatics. pp. 470-474.

[15]. Singh, S.J. and Gupta, M. (2013). Comparison of particle swarm optimization & simulated annealing for weight optimization of composite leaf spring. Inter. J. of Computational Eng. & Management. 16 (4): 14-24.

[16]. Soltani-Mohammadi, S., Safa, M. and Mokhtari, H. (2016). Comparison of particle swarm optimization and simulated annealing for locating additional boreholes considering combined variance minimization. COMPUT GEOSCI-UK. 95: 146-155.

[17]. Vanhala, H. (1997). Laboratory and Field Studies of Environmental and Exploration Applications of the Spectral Induced-polarization (SIP) Method: Synopsis. Geological Survey of Finland.

[18]. Zhdanov, M.S., Burtman, V., Endo, M. and Lin, W. (2018). Complex resistivity of mineral rocks in the context of the generalised effective-medium theory of the induced polarisation effect. Geophys Prospect. 66 (4): 798-817.

[19]. Hassan, R., Cohanim, B., De Weck, O. and Venter, G. (2005). A comparison of particle swarm optimization and the genetic algorithm. In 46th AIAA/ASME/ASCE/AHS/ASC structures, structural dynamics and materials conference (p. 1897).

[20]. Jamasb, A., Motavalli-Anbaran, S.H. and Ghasemi, K. (2018). A Novel Hybrid Algorithm of Particle Swarm Optimization and Evolution Strategies for Geophysical Non-linear Inverse Problems. Pure and Applied Geophysics. pp. 1-13.

[21]. Engelbrecht, A.P. (2007). Computational Intelligence: An introduction (second edition), John Willy and son.

[22]. Lim, S.Y., Montakhab, M. and Nouri, H. (2009). A constriction factor based particle swarm optimization for economic dispatch.

ترکیب روش‌های الگوریتم ژنتیک و بهینه‌سازی ازدحام ذرات برای بازیابی پارامترهای مدل GEMTIP از داده‌های پلاریزاسیون القائی طیفی

فریدون شریفی، علیرضا عرب‌امیری* و ابوالقاسم کامکار روحانی

دانشکده مهندسی معدن، نفت و ژئوفیزیک، دانشگاه صنعتی شاهرود، ایران

ارسال ۲۰۱۸/۱۲/۲۶، پذیرش ۲۰۱۹/۲/۱۲

* نویسنده مسئول مکاتبات: alirezaarabamiri@yahoo.com

چکیده:

تئوری محیط مؤثر قطبش القائی، مدل واهلش نوینی است که با ترکیب ریاضی ویژگی‌های ساختاری و پتروفیزیکی سنگ‌های قطبش‌پذیر در مقیاس دانه‌ها/ ادخال‌های تشکیل‌دهنده سنگ، طیف مقاومت‌ویژه/ رسانندگی مختلط آن‌ها را مدل‌سازی می‌کند. بازیابی پارامترهای مدل واهلش GEMTIP از داده‌های پلاریزاسیون القائی طیفی، به خاطر وابستگی غیرخطی داده‌های مشاهده‌ای به پارامترهای مدل و غیر یکتا بودن پاسخ مسئله، امری چالش‌برانگیز است. برای رفع این مشکلات و نیز گریز از نقاط بهینه محلی مرتبط با تابع هزینه بسیار پیچیده، می‌توان از روش الگوریتم ژنتیک استفاده کرد، اما اجرای این روش هم به صرف زمان زیادی نیاز دارد. برای رفع این کاستی می‌توان آن را با الگوریتم‌های سریع‌تر مانند الگوریتم بهینه‌سازی ازدحام ذرات تلفیق کرد. لذا هدف از انجام این پژوهش بررسی قابلیت بازیابی پارامترهای مدل واهلش GEMTIP بیضوی از داده‌های قطبش القائی طیفی با استفاده از تلفیق روش‌های الگوریتم ژنتیک و الگوریتم بهینه‌سازی ازدحام ذرات است. برای این منظور، در هر مرحله از اجرای الگوریتم، بهترین پاسخ‌های یافته شده با استفاده از روش الگوریتم ژنتیک به عنوان فضای جستجوی روش بهینه‌سازی ازدحام ذرات در نظر گرفته شده و سپس بهترین پاسخ یافته شده با استفاده از این روش، جهت به‌روزرسانی پارامترهای مدل در نظر گرفته می‌شود. نتایج مدل‌سازی نشان می‌دهد که با استفاده از روش ارائه‌شده در این پژوهش می‌توان پارامترهای مدل، به جز ثابت زمانی مرتبط با داده‌های حاوی نوفه را به خوبی بازیابی کرد که عدم بازیابی صحیح ثابت زمانی مرتبط با همبستگی منفی این پارامتر با پارامتر بیضوی ادخال‌های قطبش‌پذیر است. همچنین با استفاده از این الگوریتم، مدت زمان لازم برای همگرایی به نقطه بهینه عام، به میزان قابل‌توجهی کاهش می‌یابد.

کلمات کلیدی: تئوری محیط مؤثر قطبش القائی، الگوریتم ژنتیک، الگوریتم بهینه‌سازی ازدحام ذرات، قطبش القائی طیفی.